

# Large Fluctuations and Dynamic Phase Transition in a System of Self-Propelled Particles

F. Cagnetta,<sup>1</sup> F. Corberi,<sup>2</sup> G. Gonnella,<sup>1</sup> and A. Suma<sup>3,\*</sup>

<sup>1</sup>*Dipartimento di Fisica, Università di Bari, and Sezione INFN di Bari, via Amendola 173, 70126 Bari, Italy*

<sup>2</sup>*Dipartimento di Fisica E.R.Caianello and INFN, Gruppo Collegato di Salerno, and CNISM, Unità di Salerno, Università di Salerno, via Giovanni Paolo II 132, 8408 Fisciano (SA), Italy*

<sup>3</sup>*SISSA Scuola Internazionale Superiore di Studi Avanzati, Via Bonomea 265, 34136 Trieste, Italy*

(Received 5 July 2016; revised manuscript received 23 May 2017; published 12 October 2017)

We study the statistics, in stationary conditions, of the work  $W_\tau$  done by the active force in different systems of self-propelled particles in a time  $\tau$ . We show the existence of a critical value  $W_\tau^\dagger$  such that fluctuations with  $W_\tau > W_\tau^\dagger$  correspond to configurations where interaction between particles plays a minor role whereas those with  $W_\tau < W_\tau^\dagger$  represent states with single particles dragged by clusters. This twofold behavior is fully mirrored by the probability distribution  $P(W_\tau)$  of the work, which does not obey the large-deviation principle for  $W_\tau < W_\tau^\dagger$ . This pattern of behavior can be interpreted as due to a phase transition occurring at the level of fluctuating quantities and an order parameter is correspondingly identified.

DOI: 10.1103/PhysRevLett.119.158002

In equilibrium systems the deviations of an observable quantity from the average occur with a probability regulated by the Boltzmann-Einstein expression  $\exp\{\Delta S/k_B\}$  [1], where  $k_B$  is the Boltzmann constant and  $\Delta S$  is the entropy increase due to such a fluctuation.

In dynamical contexts one is often confronted with the related problem of finding the probability distribution of certain observables measured over a time interval  $\tau$ . A sound mathematical framework for a general description of fluctuations, which can be also applied to far-from-equilibrium systems, is provided by the large deviation theory [2]. When a large deviation principle (LDP) holds, the probability distribution  $P(W_\tau)$  of a given quantity  $W_\tau$  is characterized by a rate function  $I(W_\tau) = -\lim_{\tau \rightarrow \infty} (1/\tau) \ln P(W_\tau)$ . General predictions are in some cases available for  $I(W_\tau)$ , for example in diffusive models [3,4], where  $W_\tau$  is the particle current flowing in systems in contact with two reservoirs at different densities. Probability distributions exhibiting a nonanalytical behavior interpretable as a phase transition [4–13] have been encountered, recently attracting considerable interest.

A possibility to test and extend the above ideas in a new far-reaching context is offered by active matter. The inherently far from equilibrium systems belonging to this class, either biological or artificial in nature, display a number of nontrivial properties without analogue in passive, equilibrium materials [14–16]. A suspension of self-propelled particles, for instance, may phase separate into a dense and a gaseous phase, even in the absence of any attractive interaction [17–23]. Furthermore, active particles accumulate at boundaries [24], follow in the dilute limit a Boltzmann profile with an effective temperature when sedimenting [25–27], etc. Addressing the properties of fluctuations occurring at a mesoscopic level in these systems is fundamental for a full characterization of their functions, as, for

instance, in the case of molecular motors [28]. In the context of active Brownian motion, large deviations have been studied in experiments with an asymmetric particle interacting with a vibrated granular medium [29]. By considering the fluctuations of a quantity akin to the work defined in Eq. (2), one can test a fluctuation relation [30–32] which quantifies the relative probability of small-scale entropy consuming events that go beyond the second principle.

In this Letter, we study fluctuations in different systems of interacting active Brownian particles propelled by a force directed along their polar axis [18,19,22,33]. Specifically, we will consider the probability  $P(W_\tau)$  of the work done by the active force in a time interval  $\tau$  on each particle. Our results show that, while for values of  $W_\tau$  larger than a critical threshold  $W_\tau^\dagger$  the LDP holds, it fails for  $W_\tau < W_\tau^\dagger$  because the rate function  $I(W_\tau)$  vanishes; in this sector  $\ln P(W_\tau) \propto -W_\tau$  behaves linearly. Such a twofold behavior can be discussed in terms of a transition between a phase, for  $W_\tau > W_\tau^\dagger$ , where the particles are basically free and one, for  $W_\tau < W_\tau^\dagger$ , where they can be dragged by moving clusters. Correspondingly, an order parameter related to the relative orientation between a particle and the direction of motion of the surrounding aggregate can be defined. These results hold true for the different types of particles studied, pointing towards a general character.

We study models consisting of  $N$  particles with different shapes (for more model details, parameters used and simulation methods see the Supplemental Material (SM) [34]), either spherical colloids, dumbbells, *tetrabells*, or convex rodlike molecules (see Fig. SM5). For concreteness we describe below the case of dumbbells, a classical example of anisotropic particles which has been considered in many active matter studies [40]. Results for other kinds of particles will be presented in the SM [34].

Dumbbells are made up of two beads, a head and a tail, both having diameter  $\sigma$ . These are held together by a finitely extensible nonlinear elastic (FENE) spring. Any pair of beads interact via the purely repulsive Weeks-Chandler-Anderson (WCA) potential [41], namely, a Lennard-Jones interaction truncated at its minimum. Denoting with  $U$  the full potential (including both WCA and FENE terms), the evolution of the position  $\mathbf{x}_i$  of the  $i$ th bead is given by a Langevin equation,

$$m \frac{d^2 \mathbf{x}_i}{dt^2} = -\gamma \frac{d\mathbf{x}_i}{dt} - \nabla_i U + \mathbf{F}_a + \sqrt{2k_B T \gamma} \boldsymbol{\xi}_i(t), \quad (1)$$

where  $\gamma$  is the friction,  $\nabla_i = \partial/\partial \mathbf{x}_i$ ,  $T$  is the temperature of a thermal bath in contact with the system,  $m$  is the mass,  $\mathbf{F}_a$  is a tail-head-directed active force with constant magnitude  $F_a$ , and  $\boldsymbol{\xi}_i(t)$  is an uncorrelated Gaussian noise with zero mean and unit variance. We study a two-dimensional system. We set the parameters [42] as to have a strongly overdamped dynamics, which is realistic for microswimmers; the stiffness of the FENE springs is also strong enough [42] that the distance between the head and the tail is in practice constant and equal to  $\sigma$ . Dimensionless numbers relevant for the following are the area fraction covered by the particles,  $\phi = N\pi\sigma^2/2A$ , where  $A$  is the area of the simulation domain, and the Péclet number  $Pe = 2F_a\sigma/k_B T$  [22].

The phase diagram and other properties of this active dumbbell system have been studied in Refs. [22,43–45]. When  $\phi$  exceeds a Péclet dependent threshold, an initial homogeneous state phase separates [46]. On the other hand, for sufficiently low values of  $\phi$ , particles form small aggregates that do not coalesce. This is the situation that we find in all our simulations. In some cases, as specified in the caption of Fig. 2, the system was reported [22,46] to be slightly inside the binodal line, suggesting that macroscopic aggregation could be observed on much longer times than those addressed in this Letter.

An instance of the kind of configurations we work with is shown in Fig. 1. One observes groups of dumbbells travelling together due to steric effects and aggregates rarely exceeding ten units. For this system, under stationary conditions (see SM, Sec. IA [34]), we evaluate the observable

$$W_\tau = \frac{2}{\tau} \int_t^{t+\tau} \mathbf{F}_a(t') \cdot \mathbf{v}_i(t') dt' \quad (2)$$

representing, for each dumbbell, the work (per unit time) done by the active force. Being proportional to the time averaged projection of the center of mass velocity  $\mathbf{v}_i$  along the main direction of the dumbbell, this quantity is akin to that measured in the experiments mentioned above [29], and it also represents the entropy production for individual particles (see SM [34]). We call such an

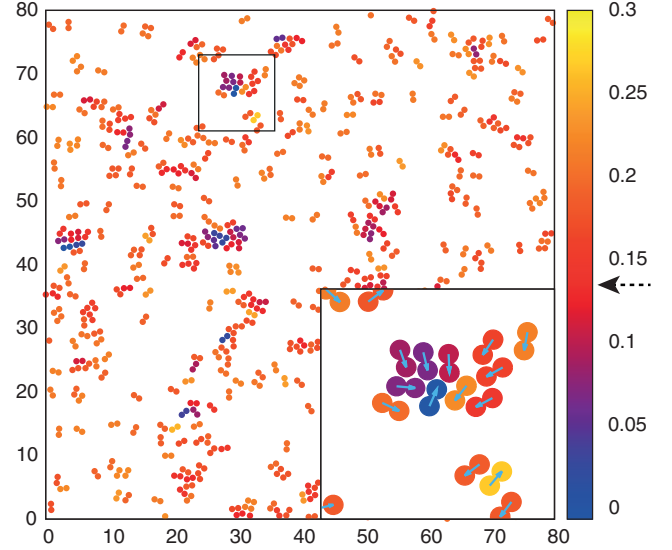


FIG. 1. A typical stationary configuration at  $\phi = 0.1$  and  $Pe = 200$ , just inside the binodal line [22], (only a portion of the system of size  $L = 200$  is shown). For each dumbbell, the color represents the value of  $W_\tau$  defined in Eq. (2) (with  $\tau = 10$ ) according to the color code in the bar on the right. The black arrow indicates the value of  $W_\tau^\dagger$ . The inset is a magnification of the highlighted box, where also the arrows representing the active force directions have been drawn [see movies M1–M5 in the SM [34] to visualize the evolution of the system (for dumbbells, colloids, tetrabells, and rods of different aspect ratio, respectively)].

observable *active work*, and the main aim of our study is to characterize the probability  $P(W_\tau)$  of its outcomes. This can be evaluated analytically only for a single non-interacting particle (see SM for details [34]). Denoting it as  $P_0(W_\tau)$ , this distribution turns out to be Gaussian with average  $\langle W_\tau \rangle_0 = 2F_a^2/\gamma$  and variance  $\langle W_\tau^2 \rangle_0 = 4F_a^2 k_B T/\tau\gamma$ . The distribution is shown in Fig. 2 (continuous black curve) where, in order to have a better representation, we plot  $\sqrt{\langle W_\tau^2 \rangle_0} P(W_\tau)$  vs  $(W_\tau - \langle W_\tau \rangle_0)/\sqrt{\langle W_\tau^2 \rangle_0}$ . In the same figure, data obtained by numerical integration of Eq. (1) for two finite particle densities are also displayed. The plots show that, irrespective of  $\phi$ , the  $W_\tau$  distribution becomes Gaussian in the small  $Pe$  limit. The curves for  $Pe = 1$  are indeed indistinguishable from the analytical ones. The same is true for any  $Pe$ , in the limit of very small area fractions (see Fig. SM2). On the other hand, the character of the distribution changes dramatically by increasing  $Pe$  at a fixed finite value of  $\phi$ . The curve remains peaked around a value close to the noninteracting one  $\langle W_\tau \rangle_0$ , is still Gaussian on the whole region to the right and immediately on the left of it, but changes abruptly as to have an approximately linear behavior of  $\ln P(W_\tau)$  for  $W_\tau$  smaller than a critical threshold  $W_\tau^\dagger > 0$ , represented by a vertical arrow in Fig. 2. This feature, which represents the central and new result of this Letter, is clearly manifest for  $Pe \gtrsim 50$ . Similar results are found for the different kind of particles before mentioned, and are shown in Fig. SM6. It is worth

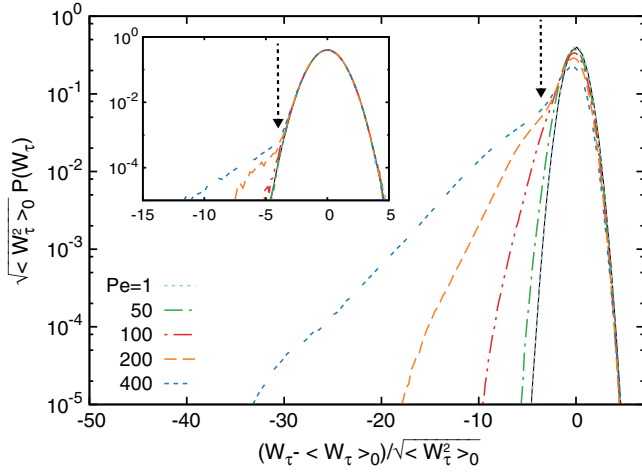


FIG. 2. Probability distributions (on log-scale) of  $W_\tau$ , with  $\tau = 20$ , for  $Pe = 1, 50, 100, 200, 400$ , at  $\phi = 0.1$  (main) and  $\phi = 0.001$  (inset). All cases fall inside the homogeneous low-density phase, except those at  $\phi = 0.1$  and  $Pe = 200, 400$  that are just inside the coexistence region. The threshold  $W_\tau^\dagger$  is signaled by vertical arrows. The continuous black curve is the analytical result for a single dumbbell (see the SM [34]).

mentioning that rods with an aspect ratio similar to the one used in this Letter lack a macroscopic phase-separation transition [47], but display an even more pronounced discontinuity at  $W_\tau^\dagger$ . This suggests that the fluctuation phenomenon we observe is not straightforwardly related to the macroscopic motility induced phase separation.

Let us now consider the effect of changing  $\tau$ . The linear decay to the left of the maximum is observable from  $\tau \sim 5$  until  $\tau \approx 1000$ . This is because for  $\tau \lesssim 5$  the distribution resembles more a Gaussian while for  $\tau \gtrsim 1000$  the tail cannot be detected with a significant statistics. In Fig. 3 we plot  $(1/\tau) \ln[P(W_\tau)/A_\tau]$  vs  $W_\tau$  for different choices of  $\tau \in [10-1000]$ , where  $A_\tau$  is the maximum of  $P(W_\tau)$  (this is done to better compare the curves at different  $\tau$ ). According to the LDP, in such a graph one should observe the data collapse of outcomes with different  $\tau$  on a master curve  $I(W_\tau)$ —the rate function. This was found in the experiments with vibrated particles [29]. Instead, what we have is something clearly different. Data collapse is only obtained for values of  $W_\tau$  larger than  $W_\tau^\dagger$ , whereas curves are well separated in the region with  $W_\tau < W_\tau^\dagger$ . These results imply that, at least in the range of times accessed in our simulations, the LDP is obeyed for  $W_\tau > W_\tau^\dagger$  but not for  $W_\tau < W_\tau^\dagger$ . In this region the large- $\tau$  limit of  $(1/\tau) \ln P(W_\tau)$  vanishes and a different scaling takes place, as discussed in the SM [34]. This implies that fluctuations are suppressed more softly for large  $\tau$  with respect to the usual case when the LDP holds. We emphasize that this anomalous behavior is not restricted to particular choices of the model parameters, but is found with the same characteristics in a whole range of densities and Péclet numbers, and for all kinds of particles considered.

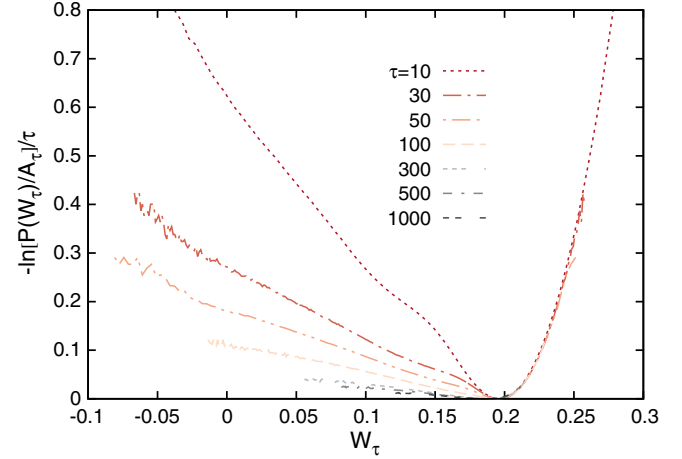


FIG. 3. The quantity  $-(1/\tau) \ln[P(W_\tau)/A_\tau]$ , is plotted vs  $W_\tau$  for different values of  $\tau$ ,  $Pe = 200$ , and  $\phi = 0.1$ .

Specifically, we observe that the breakdown of the LDP is always flanked by the appearance of the linear behavior of  $\ln P(W_\tau)$  on the left of the maximum.

In order to understand which events do contribute to the linear tails of  $\ln P(W_\tau)$ , we isolated particles trajectories with a fixed value of  $W_\tau$ . The colors in Fig. 1 represent the distribution of  $W_\tau$  in a specific realization of our system. An event with a value of  $W_\tau$  much smaller than  $W_\tau^\dagger$  (marked by a horizontal sign in the colour palette on the right) is shown in the zoomed part of the figure. One sees that the particle in the center has its polar axis pointing against a cluster moving in the opposite direction. The blue dumbbell is dragged by the cluster against its active force, resulting in a value of  $W_\tau$  significantly smaller than the average. Once the relevant mechanism is identified, a simple kinetic argument can be developed to infer the existence of a threshold  $W_\tau^\dagger$  and estimate its dependence on the model parameters. This is discussed in Sec. VI of the SM [34]. It turns out that  $W_\tau^\dagger \propto (F_a^2/\gamma)[1 - c/(D_R\tau)]$ , where  $c$  depends on the kind of active particle considered and  $D_R$  is the rotational diffusion coefficient defined in the SM [34]. This dependence has been confirmed in our simulations for all kinds of particles considered (see Fig. SM8).

Identifying the mechanism producing  $W_\tau^\dagger$  does not clarify how it originates the linear behavior of  $\ln P(W_\tau)$ . Actually, the probabilities in Fig. 2 resemble very closely those found analytically in reference statistical mechanics models, such as the Gaussian model or the zero-range process [8,9,13]. Here nonanalyticities have been discovered, and deviations corresponding to the linear tail of  $\ln P$  have been linked to a condensation transition taking place in the space of fluctuations. The system concentrates in a narrow region of phase space, similarly to what happens when a gas turns into a liquid or in Bose-Einstein condensates. Something very similar is found also in the present active matter system. Indeed, for  $W_\tau > W_\tau^\dagger$  the velocity of each dumbbell is

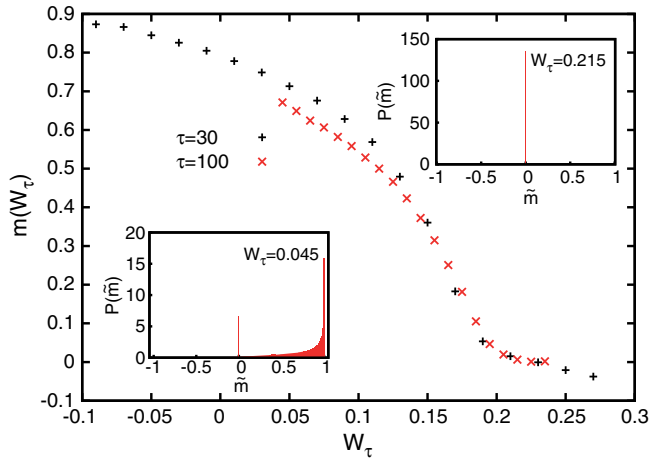


FIG. 4. The quantity  $m(W_\tau)$  is plotted vs  $W_\tau$  for  $\tau = 30$  and  $\tau = 100$  (see key), with  $Pe = 200$  and  $\phi = 0.1$ . In the two insets the histogram of the values of  $\tilde{m}$  is shown (for a case with  $W_\tau = 0.215 > W_\tau^\dagger$  on the right and with  $W_\tau = 0.045 < W_\tau^\dagger$  on the left).

symmetrically distributed around the average (as in the single particle case) and can take any possible orientation, thus filling the whole phase space. When  $W_\tau < W_\tau^\dagger$  this orientational symmetry is broken, since such velocity is set to that of the surrounding cluster.

Following this train of thought we argue that a possible order parameter should be related to the relative orientation between the dumbbell and its surroundings. Thus, calling  $\mathbf{R}_i$  the total force felt by the  $i$ th dumbbell due to interactions with other particles, and  $\theta_i$  the angle between its main axis and  $\mathbf{R}_i$ , we define a microscopic, instantaneous order parameter  $\tilde{m}(t)$ , which equals  $-\cos\theta_i$  when the dumbbell at hand is in contact with the others (let us recall that the WCA potential is truncated at distances of order  $\sigma$ , see the SM [34]), otherwise it is null. The overall order parameter  $m(W_\tau)$  is obtained by averaging  $\tilde{m}(t)$  over all the histories of time length  $\tau$  which result in an active work  $W_\tau$ .

Figure 4 shows the behavior of  $m(W_\tau)$  as a function of  $W_\tau$ . One sees that  $m$  is zero for  $W_\tau \gtrsim 0.2$ , a value that we identify with  $W_\tau^\dagger$  obtained from Fig. 2, while it increases for  $W_\tau \leq W_\tau^\dagger$  and tends to 1 at large negative  $W_\tau$ . The reason is that the instantaneous parameter  $\tilde{m}(t)$  equals 1 when the dumbbell under analysis is being pulled against its active force direction. Figure 4 clearly demonstrates that such a mechanism is effective below  $W_\tau^\dagger$ —making  $m$  finite and positive—and becomes progressively more important as  $W_\tau$  is further lowered. This behavior is robust as  $\tau$  is changed, as it is shown in Fig. 4. This is exactly the kind of property one would expect for an order parameter, with  $W_\tau$  playing the role of an external control parameter (akin to temperature), and  $W_\tau^\dagger$  that of a critical point separating a broken-symmetry phase (here for  $W_\tau < W_\tau^\dagger$ ) from a symmetric one (for  $W_\tau > W_\tau^\dagger$ ). Not only the average  $m$  has the behavior expected for an order parameter, but also its

fluctuating value  $\tilde{m}$ . The distribution of its values, shown in the insets of Fig. 4, displays indeed a single sharp peak centered around  $\tilde{m} = 0$  for  $W_\tau \geq W_\tau^\dagger$  while it develops, as soon as  $W_\tau^\dagger$  is crossed, an additional peak at  $\tilde{m} = 1$  whose height grows as  $W_\tau$  decreases, analogously to what occurs in usual equilibrium phase transitions. Here the height of the peak around  $\tilde{m} = 1$  represents the fraction of  $\tau$  for which the dumbbell has been pulled backwards by a cluster [48].

In this Letter we have highlighted the singular behavior of the large fluctuations of a quantity—the active work  $W_\tau$  done by a tagged particle—in different models representing a large class of self-propelled particle systems. We have shown that, in all cases considered, a threshold value  $W_\tau^\dagger$  exists separating regimes where fluctuations behave in a radically different way. This has been interpreted as due to a transition—occurring at the level of fluctuations—between a *gaseous* phase, where the particle internal energy is spent into self-propulsion, and one where this energy supports cluster formation. An order parameter describing the change has been also identified. The associated breakdown of the LDP reflects the importance, in terms of probabilistic weight, of clustering-related fluctuations with respect to thermal ones. For  $W_\tau < W_\tau^\dagger$ , the former are relevant to the large-scale and long-time dynamics, even for those values of the model parameters for which the whole system is in a gaseous phase.

To the best of our knowledge, this is the first evidence of a fluctuation pattern of this kind in an interacting model of active matter. In this respect, we remark that a singular distribution was also found in a model with a single active particle in an external field [49], suggesting this feature to be generic of self-propelled particles. In addition, the cruciality of interaction among particles in causing the spontaneous breaking of the orientational symmetry makes our results fundamentally different from those obtained both for the solvable cases of transitions at the fluctuating level mentioned above [8,9,13] and in the specific context of active matter.

Besides the interest of the phenomena described insofar, this study also shows that a careful analysis of nonequilibrium fluctuations may be a sophisticated tool to uncover important dynamical properties which would be missed with more conventional analytical methods. LDP violations for  $W_\tau < W_\tau^\dagger$  enhance the probability of the corresponding events, possibly with important consequences on specific properties or functions associated with the work done by active particles. This prompts further studies of the fluctuation spectra in active matter systems, particularly those of biological interest.

Simulations were run at Bari ReCaS e-Infrastructure funded by MIUR through PON Research and Competitiveness 2007-2013 Call 254 Action I. F.C. and G.G. acknowledge MIUR for funding (PRIN 2015K7KK8L and PRIN 2012NNRKA, respectively).

- \*Corresponding author.  
antonio.suma@gmail.com
- [1] L. Landau and E. Lifshitz, *Statistical Physics* (Elsevier Science, New York, 2013), Vol. 5.
- [2] H. Touchette, *Phys. Rep.* **478**, 1 (2009).
- [3] L. Bertini, A. De Sole, D. Gabrielli, G. Jona-Lasinio, and C. Landim, *Phys. Rev. Lett.* **87**, 040601 (2001); **94**, 030601 (2005).
- [4] T. Bodineau and B. Derrida, *Phys. Rev. Lett.* **92**, 180601 (2004); *Phys. Rev. E* **72**, 066110 (2005).
- [5] L. Bertini, A. De Sole, D. Gabrielli, G. Jona-Lasinio, and C. Landim, *J. Stat. Mech.* (2010) L11001.
- [6] P. I. Hurtado and P. L. Garrido, *Phys. Rev. Lett.* **107**, 180601 (2011).
- [7] G. Bunin, Y. Kafri, and D. Podolsky, *J. Stat. Mech.* (2012) L10001.
- [8] R. Harris, A. Rákos, and G. Schütz, *J. Stat. Mech.* (2005) P08003.
- [9] J. Szavits-Nossan, M. R. Evans, and S. N. Majumdar, *Phys. Rev. Lett.* **112**, 020602 (2014).
- [10] G. Gradenigo, A. Sarracino, A. Puglisi, and H. Touchette, *J. Phys. A* **46**, 335002 (2013).
- [11] A. Gambassi and A. Silva, *Phys. Rev. Lett.* **109**, 250602 (2012).
- [12] M. Filiasi, G. Livan, M. Marsili, M. Peressi, E. Vesselli, and E. Zarinelli, *J. Stat. Mech.* (2014) P09030; F. Corberi, *J. Phys. A* **48**, 465003 (2015).
- [13] M. Zannetti, F. Corberi, and G. Gonnella, *Phys. Rev. E* **90**, 012143 (2014); F. Corberi, G. Gonnella, A. Piscitelli, and M. Zannetti, *J. Phys. A* **46**, 042001 (2013).
- [14] M. C. Marchetti, J. F. Joanny, S. Ramaswamy, T. B. Liverpool, J. Prost, M. Rao, and R. A. Simha, *Rev. Mod. Phys.* **85**, 1143 (2013).
- [15] J. Elgeti, R. Winkler, and G. Gompper, *Rep. Prog. Phys.* **78**, 056601 (2015).
- [16] G. Gonnella, D. Marenduzzo, A. Suma, and A. Tiribocchi, *C. R. Acad. Sci.* **16**, 316 (2015).
- [17] J. Tailleur and M. E. Cates, *Phys. Rev. Lett.* **100**, 218103 (2008).
- [18] Y. Fily and M. C. Marchetti, *Phys. Rev. Lett.* **108**, 235702 (2012).
- [19] G. S. Redner, M. F. Hagan, and A. Baskaran, *Phys. Rev. Lett.* **110**, 055701 (2013).
- [20] J. Stenhammar, A. Tiribocchi, R. J. Allen, D. Marenduzzo, and M. E. Cates, *Phys. Rev. Lett.* **111**, 145702 (2013).
- [21] I. Buttinoni, J. Bialké, F. Kümmel, H. Löwen, C. Bechinger, and T. Speck, *Phys. Rev. Lett.* **110**, 238301 (2013).
- [22] A. Suma, D. Marenduzzo, G. Gonnella, and E. Orlandini, *Europhys. Lett.* **108**, 56004 (2014).
- [23] É. Fodor, C. Nardini, M. E. Cates, J. Tailleur, P. Visco, and F. van Wijland, *Phys. Rev. Lett.* **117**, 038103 (2016).
- [24] J. Elgeti and G. Gompper, *Europhys. Lett.* **85**, 38002 (2009); **101**, 48003 (2013).
- [25] J. Palacci, C. Cottin-Bizonne, C. Ybert, and L. Bocquet, *Phys. Rev. Lett.* **105**, 088304 (2010).
- [26] D. Loi, S. Mossa, and L. F. Cugliandolo, *Phys. Rev. E* **77**, 051111 (2008); *Soft Matter* **7**, 3726 (2011).
- [27] F. Ginot, I. Theurkauff, D. Levis, C. Ybert, L. Bocquet, L. Berthier, and C. Cottin-Bizonne, *Phys. Rev. X* **5**, 011004 (2015).
- [28] R. D. Astumian and I. Derényi, *Eur. Biophys. J.* **27**, 474 (1998).
- [29] N. Kumar, S. Ramaswamy, and A. K. Sood, *Phys. Rev. Lett.* **106**, 118001 (2011); N. Kumar, H. Soni, S. Ramaswamy, and A. K. Sood, *Phys. Rev. E* **91**, 030102 (2015).
- [30] P. I. Hurtado, C. Pérez-Espigares, J. J. del Pozo, and P. L. Garrido, *Proc. Natl. Acad. Sci. U.S.A.* **108**, 7704 (2011).
- [31] C. Ganguly and D. Chaudhuri, *Phys. Rev. E* **88**, 032102 (2013).
- [32] D. Chaudhuri, *Phys. Rev. E* **90**, 022131 (2014).
- [33] F. Peruani, A. Deutsch, and M. Bär, *Phys. Rev. E* **74**, 030904(R) (2006).
- [34] See Supplemental Material at <http://link.aps.org/supplemental/10.1103/PhysRevLett.119.158002> for simulations details, numerical and analytical results for several active Brownian particle models, which includes additional Refs. [35–39].
- [35] E. Vanden-Eijnden and G. Ciccotti, *Chem. Phys. Lett.* **429**, 310 (2006).
- [36] N. Van Kampen, *Stochastic Processes in Physics and Chemistry* (Elsevier Science, New York, 2011).
- [37] U. Seifert, *Phys. Rev. Lett.* **95**, 040602 (2005).
- [38] D. J. Evans, E. G. D. Cohen, and G. P. Morriss, *Phys. Rev. Lett.* **71**, 2401 (1993).
- [39] S. Redner, *A Guide to First-Passage Processes* (Cambridge University Press, Cambridge, England, 2001).
- [40] C. Valeriani, M. Li, J. Novosel, J. Arlt, and D. Marenduzzo, *Soft Matter* **7**, 5228 (2011).
- [41] J. D. Weeks, D. Chandler, and H. C. Andersen, *J. Chem. Phys.* **54**, 5237 (1971).
- [42] All physical quantities are expressed in reduced units of mass  $m$ , energy  $\epsilon$ , and length  $\sigma$  (the last two related to the WCA potential), which are set equal to one. The time unit is the standard Lennard-Jones time  $\tau_{LJ} = \sigma\sqrt{m/\epsilon}$ . Other important simulation parameters, in reduced units, are  $\gamma = 10$ ,  $k_B T = 0.01$  and we set  $k_B = 1$ . The simulation box is a square with side length  $200\sigma$  or more. For more informations on the potential parametrization and other simulation constants, see the SM [34].
- [43] A. Suma, G. Gonnella, G. Laghezza, A. Lamura, A. Mossa, and L. F. Cugliandolo, *Phys. Rev. E* **90**, 052130 (2014).
- [44] L. F. Cugliandolo, G. Gonnella, and A. Suma, *Phys. Rev. E* **91**, 062124 (2015); *Chaos, Solitons Fractals* **81**, 556 (2015).
- [45] M. Joyeux and E. Bertin, *Phys. Rev. E* **93**, 032605 (2016).
- [46] G. Gonnella, A. Lamura, and A. Suma, *Int. J. Mod. Phys. C* **25**, 1441004 (2014).
- [47] S. R. McCandlish, A. Baskaran, and M. F. Hagan, *Soft Matter* **8**, 2527 (2012).
- [48] It is worth noticing that  $\tilde{m}$  is strictly related to  $W_\tau$ . In fact, as shown in the SM [34], interactions between the specified dumbbell and the surrounding ones enter the quantity  $\mathbf{F}_a \cdot \mathbf{v}_i$  of Eq. (2) through the term  $[1/(2\gamma)]\mathbf{F}_a \cdot \mathbf{R}_i$ , and this in turn is proportional to  $\tilde{m}$ . Given the close relation between the order parameter  $\tilde{m}$  and  $W_\tau$ , it is not surprising that the effects of the phase transition described by  $\tilde{m}$  are so clearly displayed by  $P(W_\tau)$ .
- [49] P. Pietzonka, K. Kleinbeck, and U. Seifert, *New J. Phys.* **18**, 052001 (2016).